32nd Congress of the International Council of the Aeronautical Sciences
September 6-10, 2021
Pudong Shangri-La, Shanghai, China

Preliminary Design and Experimental Investigation of a Distributed Electric Propulsion Aircraft

Yiyuan Ma[1], Wei Zhang[1, 2], Yizhe Zhang[1], Yuelong Ma[1] & Zhiliang Bai[1]

[1]School of Aeronautics, Northwestern Polytechnical University, Xi'an, Shaanxi, 710072, PR China
[2]Key Laboratory of Aircraft Electric Propulsion Technology, Ministry of Industry and Information Technology of China, Xi'an, Shaanxi, 710129, PR China

Abstract

Distributed electric propulsion (DEP) aircraft has several potential advantages, such as improving aerodynamic performance and propulsive efficiency, making this aircraft concept one of the most promising concept for the future aviation. This paper first introduces the conceptual design considerations of DEP aircraft, including configuration, aerodynamics, structure, propulsion, control and safety. Then a 40-kg DEP Short Take-Off and Landing (STOL) demonstrator is designed and developed by using the developed initial sizing method and the aerodynamic analyses method of Vortex Lattice Method (VLM). The aerodynamic characteristics of the demonstrator are investigated and analysed in detail by using the ground mobile testing and numerical calculation methods. Finally, the DEP demonstrator is used for flight testing, and the sizing method and performance of the demonstrator are preliminarily verified. The results showed that due to the influence of the DEP system, the lift coefficient of the wing segment is increased by around 0.2 in the linear phase, and the drag coefficient is also increased due to the propulsors' incidence angle induced airflow separation.

Keywords: distributed electric propulsion, preliminary design, aerodynamic characteristics, ground mobile testing, flight testing

1. Introduction

NASA and European Union have put forward strict requirements, including reducing fuel consumption, noise and emissions, for the next-generation passenger aircraft to meet the future eco-friendly aviation goals [1]. Electric aircraft does not produce pollutants, has low noise and has almost no impact on the environment, making it is one of the important research fields of future aircraft [2]. Because the electric motor has scale-independent characteristics, it is possible to replace the traditional large engines with numerous small motors, i.e., Distributed Electric Propulsion (DEP) [3].

The application of the DEP system on passenger aircraft and Unmanned Aerial Vehicles (UAVs) has been widely studied [1]. NASA is researching a DEP blended wing body (BWB) passenger aircraft N3-X to achieve the goals of reducing fuel consumption, noise and emissions [4]. De Vries et al. [5] studied the preliminary design method of distributed propulsion aircraft, including the sizing method of wing loading and thrust-to-weight ratio and the design method for the hybrid propulsion system. Wang et al. [6] studied the sizing method of the propulsion system of distributed propulsion UAVs. Klunk et al. [7] studied the potential of using the DEP system to participate in the yaw control to reduce the vertical tail area of the aircraft and analysed it in detail with the example of ECO-150 DEP aircraft. Kerho et al. [8, 9] used computational fluid dynamics (CFD) and wind tunnel tests to study the effects of propulsors on the aerodynamic characteristics of small DEP aircraft. Pieper et al. [10] developed a dynamically-scaled DEP testbed aircraft and determined the arrangement of the propulsors using a thrust-line model. Freeman et al. [11] developed a state-space model of a DEP aircraft and simulated its six-degree-of-freedom dynamic response.

At present, the preliminary design methods of electric aircraft are mostly general conceptual design methods [12, 13] and the characteristics of the aero-propulsive coupling effects of DEP aircraft are rarely considered in these design processes. Besides, the aerodynamic characteristics of DEP aircraft and the influence of the propulsors on the aerodynamic characteristics of wings are not completely clear. Moreover, most of the DEP aircraft research is still at the theoretical analyses stage, lacking of development and flight testing to further investigate the DEP aircraft technologies and their state-of-the-art.

To this end, this paper first introduces and analyses the conceptual design considerations of DEP aircraft, and especially points out the design features of the widely concerned DEP vertical take-off and landing (VTOL) and short take-off and landing (STOL) aircraft. Then a DEP STOL demonstrator is designed and developed by using the developed initial sizing methods and the aerodynamic analyses method of Vortex Lattice Method (VLM). The aerodynamic characteristics of the DEP demonstrator are then analysed in detail by using the ground mobile experimental investigation and numerical calculations. Finally, the flight testing of the developed DEP demonstrator is carried out, and the sizing method and performance of the DEP demonstrator are preliminarily verified.

2. Conceptual Design Considerations of DEP Aircraft

2.1 Configuration Design

The electric ducted fans (EDFs) can ingest most of the boundary layer on the upper surface of the airframe when they are distributed spanwise along the wing upper trailing edge, and the boundary layer ingestion (BLI) effect will be the most significant. Therefore, most of the research on DEP passenger aircraft focus on the BWB configuration [14]. For example, NASA is researching a BWB transport aircraft with DEP for the new-generation (N+3) aviation, which is expected to reduce drag, mass and noise by installing EDFs above the airframe tail position, to meet the goals of future eco-friendly aviation [15]. Isikveren et al. [16] used the aero-propulsive coupling analysis method to study and compare the conventional wing-tube airframe, double-bubble fuselage, BWB and strut-braced wing configuration equipped with DEP systems. The results showed that the DEP BWB aircraft has the most development potential. Therefore, when there is no special design requirement, flying wing or BWB configuration can maximize the aerodynamic benefits. Besides, due to the airframe shelter effect, the DEP BWB aircraft will be quieter.

The DEP system is composed of multiple distributed propulsors, providing greater freedom for the development of novel concept aircraft. DEP VTOL and DEP STOL aircraft are the popular research fields recently [17]. This kind of aircraft is usually of canard or tandem configuration, which has high stability and safety during take-off and landing, such as Lilium jet and Vahana [4]. For this kind of aircraft, the distributed EDFs are installed on the deflectable trailing edge flap of the wing, and the thrust direction is changed by tilting the trailing edge flap to transform the aircraft flight mode. Due to the long moment arm of each propulsion group, the propulsion groups can be simplified as the four propellers of quadrotor aircraft during the take-off and landing stage. Therefore, the stability, safety and maneuverability of the DEP VTOL and DEP STOL aircraft with this configuration can meet the requirements during the take-off and landing phases.

2.2 Propulsion and Energy Systems

The conventional take-off and landing aircraft can realize the all-electric configuration by improving the propulsion system efficiency and reducing the power transmission loss. A variety of all-electric UAVs and general aviation aircraft have been developed and flied [17]. However, the battery energy density is still low, while the power demand of DEP VTOL and DEP STOL aircraft is greater. Therefore, this aircraft can choose a hybrid propulsion concept to make up for the lack of battery energy density at the state-of-the-art [4].

2.3 Yaw Control Utilizing DEP System

The propulsors of DEP aircraft are located far away from the axis of the fuselage, and the thrust difference between the propulsors on different sides of the fuselage can produce a large yaw moment. Therefore, the propulsors thrust can be used as the input of the yaw control in the flight control system, so as to partially or even completely replace the rudder [10]. Besides, if the propulsion system is allowed to participate in the flight control and stabilization of the aircraft at all times, the requirements for the vertical stabilizer will be significantly reduced, and the vertical fin can be partially or completely replaced. Therefore, incorporating the DEP system into yaw control has the potential to reduce the vertical tail area, i.e. to reduce the structural mass. However, due to the aero-propulsive coupling effect, the yaw control by the DEP system will couple the rolling motion.

2.4 Aerostructural Coordinated Design

Due to the unconventional installation position of the DEP system, the aerodynamic and structural requirements on the DEP aircraft airfoil are different from those of conventional aircraft [18]. Installing propulsors at the wing trailing edge not only increases the load on the wing structure but also transfers the thrust loads of the propulsors to the wing structure. Besides, the small thickness of the wing trailing edge also poses challenges for the installation of the EDFs' auxiliary equipment, including electronic speed controls (ESCs), power lines and cooling devices. Therefore, when determining the airfoil of a DEP aircraft, the airfoil thickness should be appropriately increased and the airfoil with a larger trailing edge angle should be selected as much as possible while meeting the aerodynamic requirements.

2.5 Safety and Reliability

The safety and reliability of the engine and its control module are some of the most important factors that affect the flight safety of aircraft. Statistical data show that 37% of UAV accidents were caused by the failure of the engine and its control module, and the reliability of the engine is the first factor affecting UAV flight safety [19]. DEP aircraft has multiple propulsors so it has a highly redundant propulsion system. The failure of individual propulsors will not significantly influence the aircraft flight safety. Therefore, it is suitable to use the DEP concept for air cargo, air taxis and other fields with high flight safety requirements.

3. Conceptual Design and Development of a DEP Demonstrator

A DEP-STOL demonstrator is designed and developed in this section to explore the technologies and characteristics of DEP aircraft through practical experiments and flight tests.

3.1 Top-Level Aircraft Requirements and Assumptions

The DEP demonstrator was designed as a testbed aircraft for research and it can also perform reconnaissance and surveillance missions. Since the demonstrator will be mainly used for flight testing, the requirement for endurance is not highly strict, so the all-electric propulsion concept was adopted. Considering that the current battery energy density is still not satisfactory, there are no additional payload requirements except for a flight control system which can be used for recording the flight data and a small camera. The top-level aircraft requirements are listed in Table 1.

Table 1 – Top-level aircraft requirements

Parameter	Value
Maximum takeoff mass, kg	40
Maximum takeoff distance, m	20
Minimum endurance, min	20
Maximum cruise speed, m/s	30
Maximum stall speed, m/s	18

For DEP aircraft, the propulsion-related parameters need to be estimated as accurately as possible to avoid large errors in the aircraft's initial sizing. The mass-specific power of the motor and electric speed controller can be taken as 5 Wh/kg and 20 Wh/kg, respectively [20]. In the DEP demonstrator development process, it was found that the current battery energy density of lithium batteries with high current discharge capability is only around 130 Wh/kg. Considering that the efficiency of EDFs is lower than 0.85 of propellers, the efficiency of EDFs was initially taken as 0.72 at the conceptual design phase.

3.2 Configuration Determination

In the conceptual design process of the demonstrator, the top-level aircraft requirements and assumptions are the basis for the initial sizing. Firstly, the concepts of the DEP system combined with four different aircraft configurations are designed separately, as shown in Fig. 1. Then the advantages and disadvantages of these four configurations are analysed in detail to determine the best configuration. In particular, the comparison of the configurations is mainly based on the practicability, realizability and design requirements of each configuration. The characteristics of each configuration and the specific tradeoff analyses for configuration selection are described as follows.

3.2.1 Conventional Configuration

The conventional configuration is represented as “a” in Fig. 1. Deflectable DEP systems are installed on the wing trailing edge to improve the STOL capability of the aircraft. The most significant advantages of this configuration are the high efficiency-cost ratio and the good flight performance proven by a large number of existing aircraft with the same configuration.

The conventional configuration features a large wing aspect ratio, giving it a high lift-to-drag ratio, resulting in a good flight performance and obvious flight endurance advantages. The conventional configuration UAV with a high wing design has a simple fuselage structure, making it convenient to install mission payloads such as electro-optical pods. Besides, the technology of conventional configuration is very mature, and the abundant reference data and engineering experience can effectively reduce the development cost. This concept requires only a little extra research and development cost for the DEP technology integration.

This configuration also has some disadvantages in that its large wingspan may not allow it to be transported using conventional small and medium-sized vehicles, which brings challenges to the frequent transportation and flight tests of the UAV. Moreover, this configuration has limited STOL performance, which may be difficult to meet the STOL design requirement.

3.2.2 Tandem Configuration

The tandem concept “b” shown in Fig. 1 is a novel aircraft configuration, replacing the traditional horizontal tails with a rear wing. Due to the large distance between the front and rear wings, the direct force control is expected to be realized through the reasonable cooperation between the control surfaces on the front and rear wings, which will greatly improve the UAV’s maneuverability and flight performance. This configuration is designed with a low front wing and a high rear wing, and the upper and lower wings are staggered to reduce the aerodynamic interference between the wings.

Both the front and rear wings of the tandem configuration produce lift, so its aerodynamic performance is better than that of conventional configuration. Since there are two wings, the wingspan of the tandem configuration is smaller than that of the conventional configuration when the wing aspect ratio is the same, which is beneficial to reduce the size of the UAV and facilitate transportation. Besides, due to the downwash effect of the front wing on the rear wing, the rear wing will stall later than the front wing, making the tandem UAV has a better stall performance. Since the deflectable DEP systems are installed on both the front and rear wings, this configuration has a better STOL performance and expected can meet the proposed STOL design requirements well.

However, since the aerodynamic interference between the front and rear wings of the tandem configuration is difficult to be estimated accurately by using semi-empirical methods, CFD and wind tunnel experiments are required for the design and development of this concept, which will increase the development cost and cycle. Moreover, the low front wing of the tandem UAV may constraint the payload arrangement in the fuselage nose.

3.2.3 Box-Wing Configuration

As shown in Fig. 1, the box-wing configuration “c” is an advanced aircraft concept in relation to the traditional cantilever wing layout of conventional and tandem configurations. Its most significant advantage is that the jointed wings are used to reduce the wing bending moment and shear force, decreasing the wing structural weight and material requirements compared to the conventional cantilever wing concept. Deflectable DEP systems installed only on the front wing which has a low sweep angle.

Since the box-wing configuration is evolved from the tandem configuration, this concept has both the advantages and disadvantages of the tandem configuration, such as ease of transportation, good aerodynamic performance and good stall performance and so on. Moreover, the box-wing configuration is conducive to reducing the induced drag due to the installation of endplates at the wingtips, thus improving the aircraft lift-to-drag ratio.

Nevertheless, the disadvantages of the tandem configuration also apply to the box-wing configuration. For example, the research and development cost is high and the payload arrangement space is limited. Besides, in order to connect the wingtips of the front and rear wings, the rear wing of the box-wing configuration has a large forward-swept angle, which makes it inappropriate to install the DEP system on its rear wing, resulting in its STOL performance inferior to that of the tandem concept.

3.2.4 BWB Configuration

With the development of the flight control technology, the BWB configuration has been widely used because both its fuselage and wing can produce considerable lift contribution and has smaller parasite drag. As shown in Fig. 1, the airframe trailing edge of BWB concept "d" is designed without a sweep angle for the arrangement of the DEP system.

Because the BWB aircraft airframe can also produce a lot of lift, the size of the aircraft is smaller than that of the conventional configuration. Besides, the BWB concept has fewer components, less drag and a high lift-to-drag ratio, so it can carry more payloads. However, due to its static instability, the BWB UAV needs a specially developed flight control system to ensure its flight stability. Most importantly, the STOL performance of the fly-wing UAV is poor because the DEP system can only be installed on the airframe trailing edge, which cannot contribute to the vertical direction thrust.

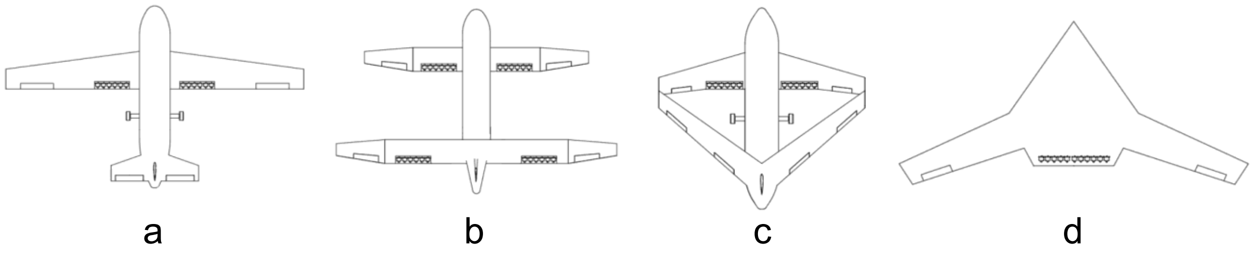

Figure 1 – Initially proposed configurations.

3.2.5 Configuration Selection

Corresponding to the above analyses of the advantages and disadvantages of these four initial proposed configurations, and based on the practicality and realizability of each design and the fulfillment of the design requirements, the UAV's configuration is selected and determined as follows.

As this UAV will be used as a demonstrator for DEP-related technologies, including the DEP control technology, the BWB concept was firstly excluded due to the complexity of its flight control system development. Considering that the UAV as a demonstrator needs to be transported for flight testing frequently, the box-wing and tandem configurations are preferred due to their smaller size. Then, according to the STOL requirement listed in Table 1, the tandem configuration is final selected for the demonstrator.

The thrust of the DEP system is transmitted through the wing structure, meaning that the strength and stiffness of the wing structure need to be improved, resulting in an increased aircraft structural mass. The twin-fuselage configuration has the advantages of reducing the wing blending moment to reduce the wing structural mass and is conducive to the arrangement of the numerous batteries and electronic devices [21, 22]. However, the twin-fuselage configuration will also increase the interference drag of the wing and fuselages. Considering the DEP systems arrangement, the twin-fuselage configuration is used for the demonstrator, the UAV's final configuration is shown in Fig. 4.

The DEP system of the demonstrator is composed of 24 EDFs. As shown in Fig. 2, six EDFs are taken as a group and the four groups are installed in different positions of the wings. The DEP systems are installed on the demonstrator's wing flaps, and the lower lip of the propulsor is set close to the wing's upper surface to ingest the wing boundary layer. During the STOL phase, the flaps of the inboard wings tilt together with the propulsors mounted on them to provide vertical direction thrust, while the horizontal-direction thrust is generated by the DEP systems installed on the outboard of the rear wing.

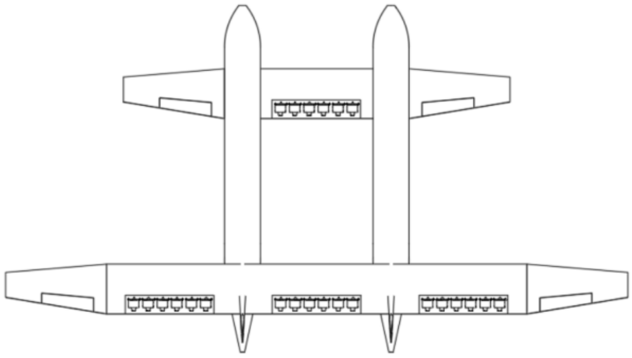

Figure 2 – Final configuration of the demonstrator.

3.3 Initial Sizing and Analyses

The wing loading and thrust-to-weight ratio need to be estimated for the conceptual design. In the initial sizing, the wing loading and thrust-to-weight ratio need to be determined according to the different aircraft performance constraints corresponding to the top-level aircraft requirements. According to the DEP aircraft initial sizing methodology presented in Ref. [23], the wing loading and thrust-to-weight ratio of the UAV were estimated with respect to the cruise speed, climb rate, takeoff distance and stall speed, respectively, and the thrust-to-weight ratio was taken as the maximum value of 1.0644 and the wing loading was taken as the minimum value of 18.6 kg/m^2.

For the aerodynamic analyses of the DEP demonstrator at the conceptual design phase, the CFD method is not appropriate due to its time-consuming. A combination of the semi-empirical method and VLM was used to analyse the DEP demonstrator's aerodynamic performance. Since the aerodynamic influence of the DEP system on the aircraft airframe cannot be introduced in the VLM tool directly, the clean configuration (i.e., without the DEP system) was used for the analyses. It can be predicted that the aerodynamic results will be worse than that of the actual situation due to the lacking of BLI effect, but this effective method is only used at this initial sizing stage, which will be modified by CFD calculations, wind tunnel experiments and ground mobile tests in the subsequent design and development phase. The clean configuration of the demonstrator is modeled by OpenVSP, as shown in Fig. 3, and the aerodynamic analyses is carried out by the VSPAERO. Several important aerodynamic parameters are listed in Table 2.

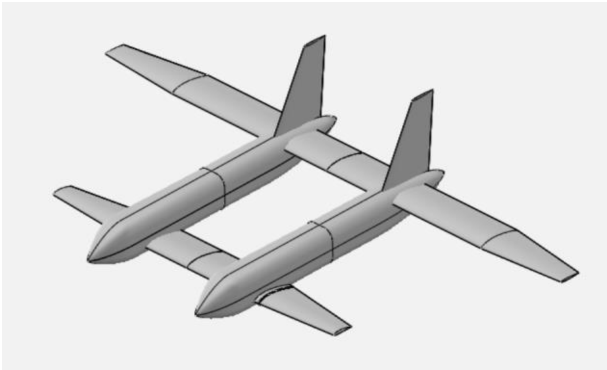

Figure 3 – Clean configuration of the demonstrator.

Table 2 – Aerodynamic performance

Parameter	Value
Max lift coefficient	1.5
Min drag coefficient	0.045
Min drag lift coefficient	0.33
L/D cruise	9.6

The initial sizing method of DEP aircraft, including mass properties and endurance, was developed by Ma et al. [24]. The parameters listed in Table 1 and estimated above are used for the initial sizing of the DEP demonstrator, and the initial sizing results are shown in Fig. 4. The initially estimated endurance of the DEP-STOL demonstrator is 18.14 min, which is slightly lower than that of the design requirement. Considering that the DEP demonstrator is mainly developed for flight testing purposes, this performance is considered to be acceptable.

Mass	40 kg		Front-wing	Rear-wing
		Airfoil	NACA 4415	NACA 4415
Length	2.43 m	Area (m^2)	0.804	1.368
Span	4.39 m	Span (m)	2.74	4.388
Height	1.08 m	Dihedral (deg)	0	0
		Aspect Ratio	8.93	13.60
P/W	0.497 W/g	Taper Ratio	0.5	0.5
Cruise Speed	25 m/s	Root Chord (m)	0.345	0.345
Stall Speed	15 m/s	Tip Chord (m)	0.173	0.173
Endurance	18.14 min	MAC (m)	0.311	0.325

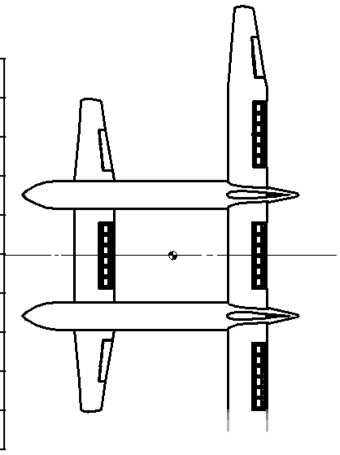

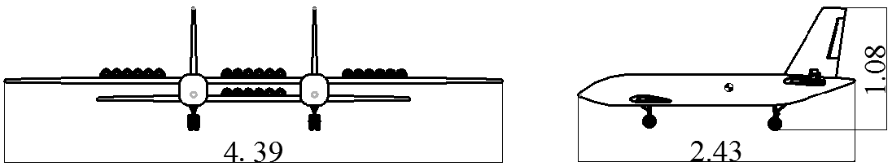

Figure 4 – Initial sizing results of the DEP UAV.

3.4 Manufacturing Process

Computer-Aided Design (CAD) was used to generate the detailed geometry of the demonstrator and to model the airframe structure components, which is used for components manufacturing.

Aluminum alloy is used for the reinforced wing ribs and landing gears of the demonstrator, which was formed and cut by using a Computer Numerical Control (CNC) machine according to the CAD outputs. Carbon composite material with aramid honeycomb core is utilized for the other structure components, such as ribs, frames and floors. The demonstrator manufacturing begins from the hand lay-up of the impregnated carbon cloth and honeycomb core into the processed mold, and then they are cured through the vacuum bagging process.

The electronic devices of the demonstrator, including EDFs, electric speed controllers, servo actuators and batteries, are then installed to the corresponding positions of the wing or fuselage. The EDFs are mounted on the wing flaps through supports, in which the electric speed controllers are placed inside, as shown in Fig. 5. The flap with EDFs mounted is connected to the wing through a shaft, and the flap together with EDFs tilt as the shaft rotates, as shown in Fig. 6. The manufactured demonstrator is shown in Fig. 7.

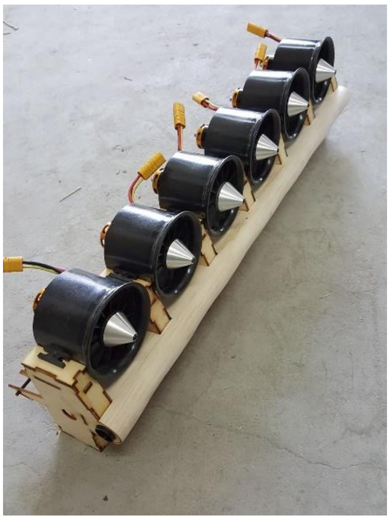

Figure 5 – Flap with EDFs mounted.

Figure 6 – Wing with the DEP system installed.

Figure 7 – The DEP demonstrator.

4. Aero-Propulsive Coupling Analyses

The propulsors distributed over the wing can improve the lift coefficient and reduce the drag coefficient of the wing through the BLI effect [25]. However, if it cannot be specifically quantified, it will pose a challenge to the flight safety and flight control system development for such UAVs. In this section, the aerodynamic characteristics of the demonstrator are analysed using numerical calculations, which are validated by ground mobile testing.

The ground mobile testing system of the demonstrator is shown in Fig. 8, a measurement platform with force sensors is mounted on top of a vehicle for experiments, through which the DEP demonstrator is connected to it. The experimenter drives the vehicle to simulate the flight speed of the demonstrator, and the measurement system records data from the demonstrator, such as the aerodynamics and current and voltage of the DEP system. The ground mobile testing investigation can not only provide the crucial data for the researchers to conduct the aircraft first flight but also provide the important reference information for the aircraft dynamic modeling and the flight control system development, which is of great significance for the unconventional aircraft concepts design and development.

Figure 8 – Ground mobile testing system.

There is always a lot of uncertainties when conducting practical experiments, and due to the limitations of the experimental system, it is not possible to measure the important parameter drag of the demonstrator. Therefore, although the more realistic aerodynamic data of the studied demonstrator can be obtained by the ground mobile testing, the CFD method is used to analyse the aerodynamics and flow fields of the demonstrator's wing with EDFs mounted, and the results are validated by the ground mobile testing results.

The structural mesh is used to solve the Navier-Stokes equations. The wing segment and the EDFs are the same as those of the demonstrator. The surface mesh of the half-model is shown in Fig. 9. The number of mesh points near the leading edge, trailing edge and EDFs is increased respectively, and the total number of the grid cells is around 6 million. The thrust effect of EDFs is simulated by setting pressure jump for the boundary condition of the fan face and take the pressure jump as the static thrust of the EDF at the corresponding throttle state. The Spalart-Allmaras model is used for the turbulence simulation, and the incoming velocity is 20 m/s.

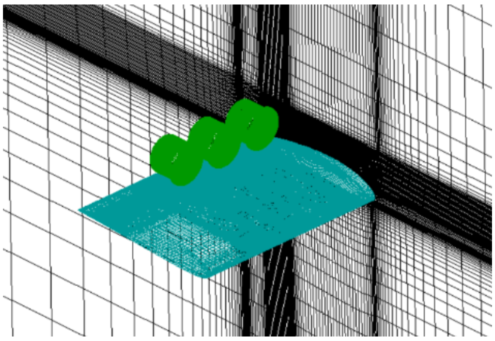

Figure 9 – The surface mesh of the wing segment.

The ground mobile testing results were utilized to verify the presented CFD method. During the ground mobile tests, the angle of attack and speed of the demonstrator is taken as the fixed value. The lift data of the demonstrator at different throttle states are measured, and the component of thrust in the lift direction caused by the incidence angle of the front and rear wings and the pitch angle of the demonstrator was subtracted. Then, by comparing with the lift at the zero-thrust state, the lift coefficient increment due to the thrust generated by the DEP system at different throttle states can be obtained. This method does not change the angle of attack of the demonstrator, so it does not introduce the lift increment due to the unrelated components such as fuselages and outboard wings.

Figure 10 shows the comparison of numerical calculations and ground mobile tests when the angle of attack is 5 degrees and the flow velocity is 20 m/s. The lift coefficient increment of the CFD method is larger than that measured from the ground testing, which is due to the static thrust of the EDF was set for the fan face in the numerical calculations, which is higher than that of the practical situations, resulting in an increase in the wing lift coefficient increment greater than that of the ground mobile testing. However, the trends of the lift coefficient increment with respect to the changes of percent throttle calculated by numerical calculations and measured by ground mobile tests are consistent, which proves that the CFD method presented in this paper is feasible.

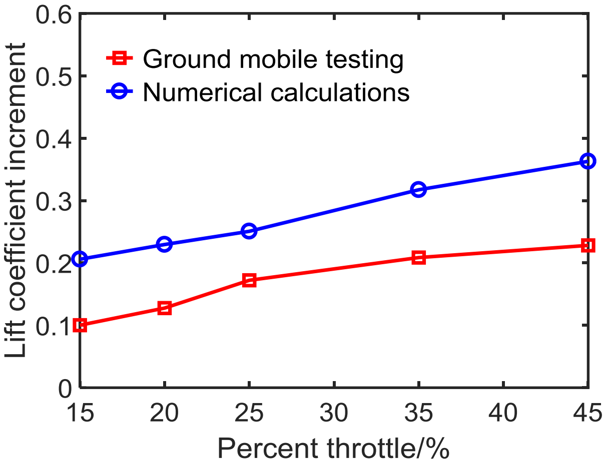

Figure 10 – Validation of the CFD calculations.

The surface streamlines of the ground mobile testing are shown in Fig. 11, and the angle of attack is 5 degrees and the flow velocity is 20 m/s. As shown in Fig. 11, the streamlines on the wing surface become more uniform and orderly as the propulsors' thrust increases.

It should be noted that the airflow separation occurs on the upper surface of the wing trailing edge because the incidence angle of the propulsors on the wing is zero degrees, i.e., it is parallel to the wing chord, so there is an angle between the airflow jetting backward from the propulsors and the upper surface of the wing trailing edge. The jet speed of the propulsors is fast, while the airflow velocity at the upper surface of the trailing edge is relatively slow. Therefore, there is a significant pressure difference between the two airflows, making it difficult of the airflow on the wing trailing edge to continue to flow stably along the wing surface, and flow separation occurs, reducing the lift generation of the wing trailing edge and increase the pitching moment of the wing. In the following design phase, the propulsors should be designed with an appropriate incidence angle so that its jet is close to or tangent to the wing trailing edge, so as to avoid the lift loss caused by the airflow separation. However, the propulsors with an incidence angle will introduce additional pitching moments for the aircraft due to the thrust, which will bring new problems to the stability and control of the aircraft. Therefore, the installation of propulsors is not only a problem of aerodynamics but also a coordinated design by balancing the needs and constraints of various disciplines in the preliminary design stage.

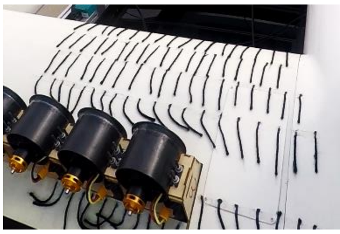
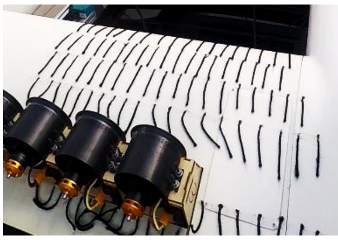
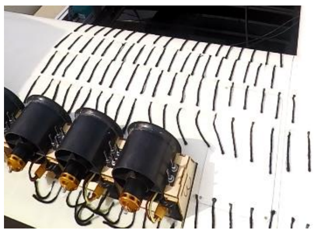

a) T=0 b) T=15% c) T=20%

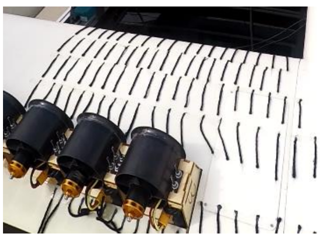
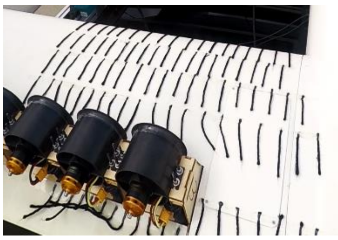


d） T=25%　　e） T=35%　　f） T=45%

Figure 11 – Wing surface airflow of ground mobile tests.

The same mesh generation method and solver setting method were used to analyse the clean wing (i.e., without propulsors), and the results are compared with that of the DEP wing. As shown in Fig. 12, the lift coefficient increment due to the DEP system is around 0.2 in the linear phase, indicating that the BLI effect of the DEP system on the wing airflow can significantly improve the lift coefficient of the wing. Besides, the DEP system also delays the separation of the airflow on the wing upper surface and delays the stall significantly. It is worth noting that in the negative angle condition, the wing with DEP mounted can still produce a certain amount of lift at a large negative angle, which is due to the BLI effect of the propulsors on the airflow near the wing upper surface.

As shown in Fig. 13, the drag coefficient of the wing with DEP installed is greater than that of the clean wing, especially at a high angle of attack. This is due to the unreasonable design of the propulsors incidence angle on the wing, resulting in airflow separation on the upper surface of the wing trailing edge, increasing the pressure drag.

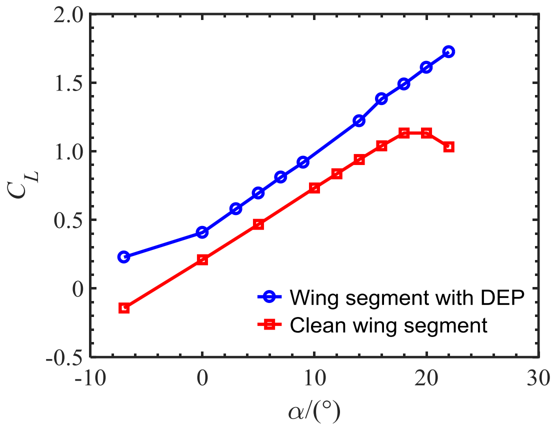

Figure 12 – Curves of lift coefficient vs. angles of attack.

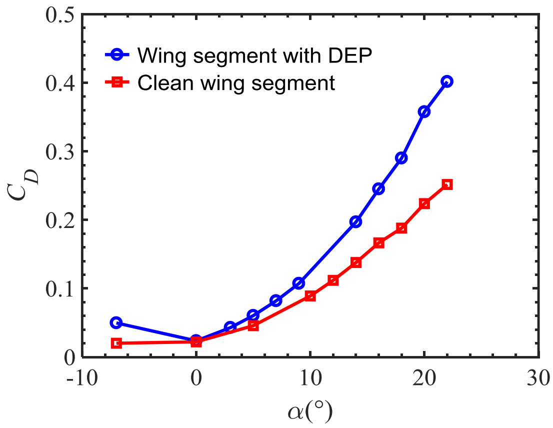

Figure 13 – Curves of drag coefficient vs. angles of attack.

The streamlines of the wing segment at the 18 degrees of attack are shown in Fig. 14. At this angle of attack, the airflow on the upper surface of the clean wing segment begins to separate from the trailing edge and expand forward, and the wing begins to stall. However, at this high angle of attack, the airflow on the DEP wing segment upper surface has not been separated in a large range due to the ingesting effect of the EDFs, and only the airflow separation induced by the propulsors' jet appears at the wing trailing edge.

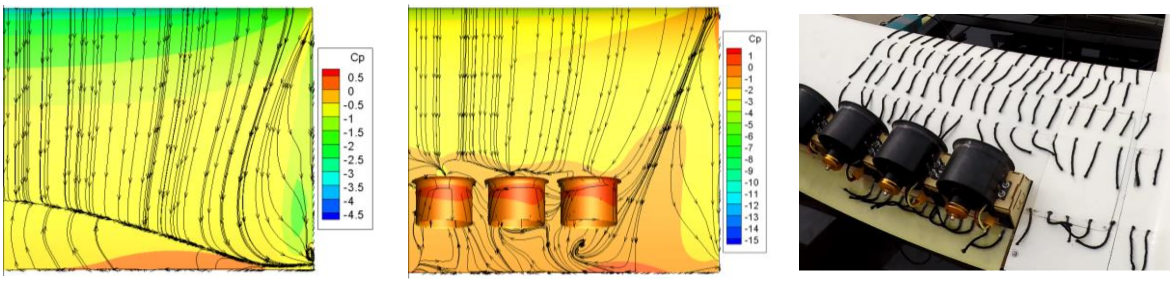

Clean wing | Wing with EDFs mounted | Ground mobile testing

Figure 14 – Streamlines on the wing surface at 18 degrees of attack.

5. Flight Testing of the DEP Demonstrator

After completing the ground mobile tests and evaluating the stability and control of the DEP demonstrator, flight testing can be conducted. The initial sizing method for DEP aircraft utilized in this paper and the feasibility and performance of the designed DEP demonstrator can be verified by practical flight data. So far, the development of the flight control system of the DEP-STOL demonstrator has not been finished, so the flight testing is carried out by using conventional takeoff and landing approach. The flight testing of STOL performance will be conducted after finishing the development of the flight control system. During the flight testing, the demonstrator is controlled manually through a radio-controlled (R/C) receiver. A picture of the DEP demonstrator during cruise is shown in Fig. 15, and some of the recorded flight data of a flight test are shown in Fig. 16 and 17.

Figure 15 – Flight testing of the DEP demonstrator.

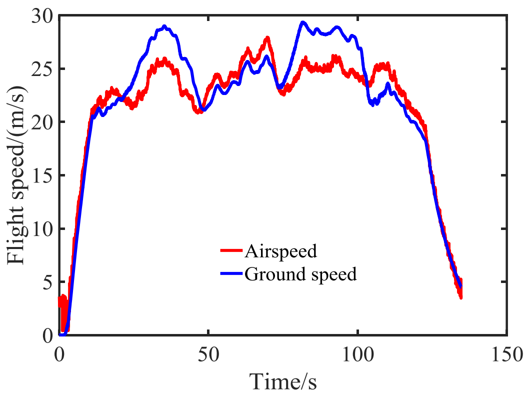

Figure 16 – Flight speed data records.

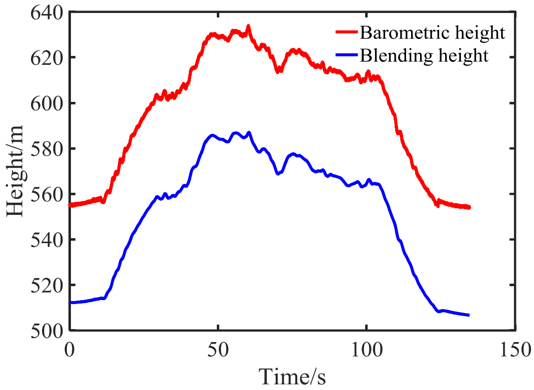

Figure 17 – Flight altitude data records.

Since the current flight testing was manually controlled, it is difficult to accurately analyse the stability and control characteristics of the DEP demonstrator. Simple maneuvers were carried out through manual control to initially explore and validate the stability and control characteristics of the DEP demonstrator. The demonstrator was manually controlled for pitching maneuver, and then its stability characteristics could be initially tested by observing its natural response. As shown in Fig. 18 to 20, three times stability tests were performed, and the DEP demonstrator returned to the horizontal flight state immediately after inputting the perturbation without significant oscillations, proving the developed DEP demonstrator has good stability characteristics.

Figure 18 –Pitch control and response snapshots of the DEP demonstrator (from left to right).

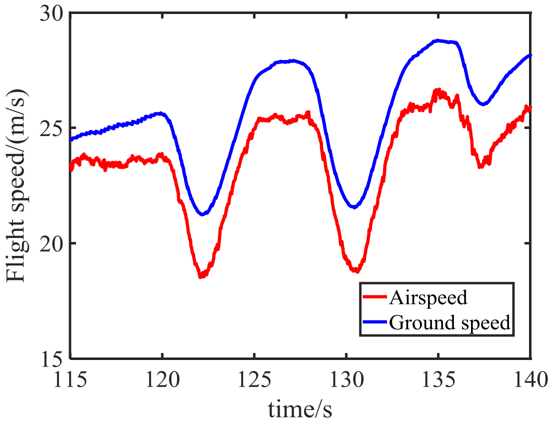

Figure 19 –Velocity response with three times input perturbations.

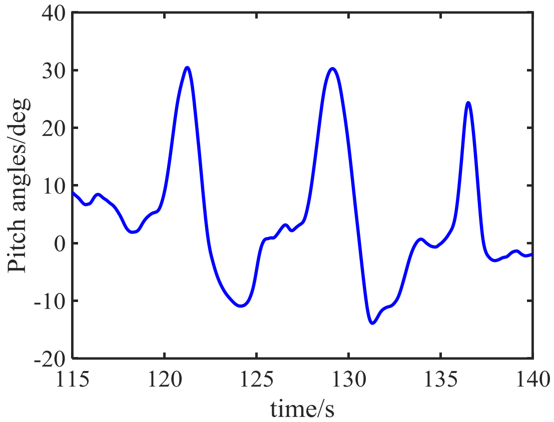

Figure 20 –Pitch angles response with three times input perturbations.

Through the flight testing, it is proved that the DEP demonstrator can complete each flight process and has a good maneuverability and stability, and the feasibility of the initial sizing method used in this research and the conceptual design of the DEP demonstrator are initially verified. Because the demonstrator is controlled manually, the fluctuation of flight data is large, which is not conducive to system identification and accurate dynamic modeling. However, some important and useful information can still be initially extracted from the flight data obtained at this stage for preliminary analyses and verification. As listed in Table 3, the cruise speed and stall speed of the demonstrator meet the top-level requirements well. In the next step, after the development of the flight control system, the autopilot will be used to control the demonstrator for more flight tests and system identification.

Table 3 – Flight testing data

Parameter	Value
Takeoff speed, m/s	19.0
Cruise speed, m/s	23.5
Landing speed, m/s	17.0
Cruise angle of attack, degrees	3.0
Takeoff running distance, m	67.5
Landing running distance, m	129.64

6. Conclusions

This paper presents the design, development and experimental investigation of a DEP demonstrator. The conceptual design considerations for DEP aircraft were first introduced and described in terms of several disciplines, respectively. Then according to the top-level aircraft requirements, a 40 kg DEP-STOL tandem wing and twin-fuselage configuration UAV was designed and developed as a demonstrator for the DEP technology exploration. The developed initial sizing methods for DEP aircraft and the aerodynamic analyses method of VLM were utilized for the conceptual design of the demonstrator. Then the demonstrator was installed on top of a vehicle for the ground mobile testing, and the numerical calculation method was carried out for the demonstrator's wing segment and validated by the ground mobile testing data. In the linear phase, the increment of the induced lift coefficient due to the DEP system on the wing segment is around 0.2, and the wing drag is also increased due to the propulsor's incidence angle induced airflow separation. If the incidence angle of the propulsors is not well-designed, airflow separation may occur at the wing trailing edge, which will decrease the aerodynamic performance of the wing. Finally, the flight testing was carried out for the DEP demonstrator, and some crucial flight performance of the demonstrator, including cruise speed, stall speed and so on, were preliminary validated.

7. Contact Author Email Address

Prof. Dr. Wei ZHANG
Deputy Director of Experimental Aircraft Design & Test Technique Lab. of NPU
School of Aeronautics
Northwestern Polytechnical University
YOUYI XILU 127#
710072 XI'AN, CHINA
Email: weizhangxian@nwpu.edu.cn

8. Copyright Statement

References

[1] Kong X, Zhang Z, Lu J, Li J and Yu L. Review of electric power system of distributed electric propulsion aircraft. *Acta Aeronautica et Astronautica Sinica*, Vol. 39, No. 1, pp 021651, 2018.

[2] Huang J and Yang F. Development and challenges of electric aircraft with new energies. *Acta Aeronautica et Astronautica Sinica*, Vol. 37, No. 1, pp 57-68, 2016.

[3] Gohardani A S, Doulgeris G and Singh R. Challenges of future aircraft propulsion: A review of distributed propulsion technology and its potential application for the all electric commercial aircraft. *Progress in Aerospace Sciences*, Vol. 47, No. 5, pp 369-391, 2011.

[4] Kim H D, Perry A T and Ansell P J. A review of distributed electric propulsion concepts for air vehicle technology. *2018 AIAA/IEEE Electric Aircraft Technologies Symposium*, Cincinnati, USA, pp 4998, 2018.

[5] de Vries R, Brown M and Vos R. Preliminary sizing method for hybrid-electric distributed-propulsion aircraft. *Journal of Aircraft*, Vol. 56, No. 6, pp 2172-2188, 2019.

[6] Wang S, Economou J T and Tsourdos A. Indirect engine sizing via distributed hybrid-electric unmanned aerial vehicle state-of-charge-based parametrisation criteria. *Proceedings of the Institution of Mechanical Engineers, Part G: Journal of Aerospace Engineering*, Vol. 233, No. 14, pp 5360-5368, 2019.

[7] Klunk G T and Freeman J L. Vertical tail area reduction for aircraft with spanwise distributed electric propulsion. *2018 AIAA/IEEE Electric Aircraft Technologies Symposium*, Cincinnati, USA, pp 5022, 2018.

[8] Kerho M F. Aero-propulsive coupling of an embedded, distributed propulsion system. *33rd AIAA Applied Aerodynamics Conference*, Dallas, USA, pp 3162, 2015.

[9] Perry A T, Ansell P J and Kerho M F. Aero-propulsive and propulsor cross-coupling effects on a distributed propulsion system. *Journal of Aircraft*, Vol. 55, No. 6, pp 2414-2426, 2018.

[10] Pieper K, Perry A, Ansell P and Bretl T. Design and development of a dynamically, scaled distributed electric propulsion aircraft testbed. *2018 AIAA/IEEE Electric Aircraft Technologies Symposium*, Cincinnati, USA, pp 4996, 2018.

[11] Freeman J L and Klunk G T. Dynamic flight simulation of spanwise distributed electric propulsion for directional control authority. *2018 AIAA/IEEE Electric Aircraft Technologies Symposium*, Cincinnati, USA, pp 4997, 2018.

[12] Finger D F, Braun C and Bil C. An initial sizing methodology for hybrid-electric light aircraft. *2018 Aviation Technology, Integration, and Operations Conference*, Atlanta, USA, pp 4229, 2018.

[13] Wang S, Economou J T and Tsourdos A. Design of a distributed hybrid electric propulsion system for a light aircraft based on genetic algorithm. *AIAA Propulsion and Energy 2019 Forum*, Indianapolis, USA, pp 4305, 2019.

[14] Ashcraft S W, Padron A S, Pascioni K A, Stout G W, Huff D L. Review of propulsion technologies for N+ 3 subsonic vehicle concepts. *NASA/TM—2011-217239*, 2011.

[15] Kim H and Liou M S. Flow simulation of N2B hybrid wing body configuration. *50th AIAA aerospace sciences meeting including the new horizons forum and aerospace exposition*, Nashville, USA, pp 0838, 2012.

[16] Isikveren A T, Seitz A, Bijewitz J, Hornung M, Mirzoyan A, Isyanov A, Godard J L, Stückl S, van Toor J. Recent advances in airframe-propulsion concepts with distributed propulsion. *29th Congress of the International Council of the Aeronautical Sciences*, St. Petersburg, Russia, 2014.

[17] Brelje B J and Martins J R R A. Electric, hybrid, and turboelectric fixed-wing aircraft: A review of concepts, models, and design approaches. *Progress in Aerospace Sciences*, Vol. 104, pp 1-19, 2019.

[18] Ma R and Wu J. Multipoint and multi-objective optimization of airfoil considering boundary layer ingestion. *Proceedings of the 2018 Asia-Pacific International Symposium on Aerospace Technology (APISAT 2018),* Chengdu, China, Vol. 459, pp 61-73, 2019.

[19] Cai Z, Yang L, Wang Y and Li X. Analyses for whole airspace flight key factors of unmanned aerial vehicles. *Journal of Beijing University of Aeronautics and Astronautics*, Vol. 37, No. 2, pp 175-184, 2011.

[20] Finger D F, Braun C and Bil C. Impact of electric propulsion technology and mission requirements on the performance of VTOL UAVs. *CEAS Aeronautical Journal*, Vol. 10, No. 3, pp 827-843, 2019.

[21] Jong T and Slingerland R. Analyses of the twin-fuselage configuration and its H-cabin derivative. *AIAA's 3rd Annual Aviation Technology, Integration, and Operations (ATIO) Tech*, Denver, USA, pp 6811, 2003.

[22] Udin S V and Anderson W J. Wing mass formula for twin fuselage aircraft. *Journal of Aircraft*, Vol. 29, No. 5, pp 907-914, 1992.

[23] Ma Y, Zhang W, Zhang X, Zhang X, Ma Y and Guo Z, Primary parameters design method for distributed electric propulsion unmanned aerial vehicle. *Journal of Northwestern Polytechnical University*, Vol. 39, No. 1, pp 27-36, 2021.

[24] Ma Y, Zhang W, Zhang Y, Zhang X and Zhong Y. Sizing method and sensitivity analyses for distributed electric propulsion aircraft. *Journal of Aircraft*, pp 1-12, 2020.

[25] Ma Y, Zhang W, Zhang Y, Li K and Wang Y. Effects of distributed propulsion crucial variables on

aerodynamic and propulsive performance of small UAV," *Proceedings of the 2018 Asia-Pacific International Symposium on Aerospace Technology (APISAT 2018),* Chengdu, China, Vol. 459, pp 1535-1550, 2019.